Effect of polymer compatibility on surface enrichment in polymer blends

Panos Sakellariou
ICI Paints, Research Department, Wexham Road, Slough SL2 5DS, UK
(Received 1 September 1992; revised 11 December 1992)

The surface composition of blends of poly(ethylene oxide) (PEO) with polystyrene (PS), poly(methyl methacrylate) (PMMA) and random copolymers of styrene and methyl methacrylate (MMAS) has been studied as a function of blend and copolymer compositions. In the case of homopolymer blends, only the incompatible blend PEO/PS showed significant surface enrichment in PS following annealing at temperatures above the T_g of the two constituents and the T_m of PEO. The compatible system PEO/PMMA presented a mixed surface. Surface enrichment in the MMAS copolymers was observed in all PEO/MMAS blends with styrene contents in excess of 2% w/w. This has been attributed to the incompatibility between the PEO and the MMAS copolymers as shown by the ternary phase diagram PEO/MMAS/$CHCl_3$ and the melting-point depression of the PEO-rich phases with varying copolymer composition and concentration. Angle-dependent X-ray photoelectron spectroscopy provided an indication of the depth–concentration profile of the blend. The results of these measurements demonstrate that increased styrene content in the MMAS copolymer produces deeper concentration profiles, which reached down to 69 Å from the surface. Mean-field calculations of the depth–concentration profile for a selected system gave very good agreement with the experimental data.

(Keywords: blends; compatibility; surface enrichment; X-ray photoelectron spectroscopy; depth–concentration profile)

INTRODUCTION

In the past 10 years, increasing attention has been directed towards the surface properties of polymer blends. The topic holds great significance in both academic and industrial terms. Polymers offer the unique opportunity of studying critical wetting phenomena in mixed systems by virtue of the capability to vary, in a controlled fashion, the length of the chains while keeping the basic segment–segment interactions constant[1,2]. From the industrial point of view, controlled surface modification of polymer blends allows decoupling of the surface properties of a material from its bulk properties. This has major implications in a wide range of materials as diverse as paints and biocompatible materials.

The Gibbs adsorption isotherm expresses clearly that any differential in the surface energy of the constituents of a multicomponent system, $d\gamma$, results in relative enrichment of the air interface in the lower-surface-energy material:

$$d\gamma = \sum_i \Gamma_i \mu_i$$

where μ_i is the chemical potential and Γ_i is the surface excess of species i.

O'Malley and coworkers[3–5] have studied the surface of di- and triblock copolymers of polystyrene (PS) and poly(ethylene oxide) (PEO) and the corresponding homopolymer blend. In all cases they observed relative surface enrichment of the air interface in the lower-surface-energy constituent, PS. Schmitt and coworkers[6] made a similar observation in blends of polycarbonate (PC) and poly(dimethyl siloxane) (PDMS), reporting an eight-fold increase in the PDMS concentration at the surface. Gardella *et al.*[7] extended the range of systems studied to poly(ε-caprolactone)/poly(vinyl chloride) (PCL/PVC) blends and found that the surface composition was dependent on polymer molecular weight and degree of crystallinity. In the case of poly(methyl methacrylate)/poly(vinyl chloride) (PMMA/PVC) blend, surface enrichment in PMMA was observed when the blends were cast from tetrahydrofuran (THF), while in the case of methyl ethyl ketone (MEK) the surface composition was similar to that of the bulk[8]. This was attributed to the phase separation in the former system compared to the fully compatible system obtained with the latter one. Surface enrichment in the lower-surface-energy component has also been reported in blends of poly(α-methylstyrene) with poly(2-hydroxyethyl methacrylate)[9], poly(ether sulfone) with poly(ethylene oxide)[10] and polystyrene/poly(vinyl methyl ether) (PS/PVME)[11]. Surface enrichment has been observed even with very small differences in the surface energy of the blend constituents, as in the case of PS mixed with deuterated PS[12,13].

From the theoretical treatments[1,2] and the available experimental data, it is clear that the compatibility between the blend constituents plays a significant role in surface enrichment. In this paper we address this issue in blends of PEO with PS, PMMA and random copolymers of styrene with methyl methacrylate (MMAS). It is well established that PEO is compatible with PMMA[13–16] and incompatible with PS[17]. PS, PMMA and MMAS are the lower-surface-energy components

0032-3861/93/163408-08

and are expected to enrich the surface. We have studied the effect of incompatibility on surface enrichment by studying the surface of the two homopolymer blends, as representatives of the two extremes, and a range of MMAS copolymers with varying composition. The ratio of favourable/unfavourable interactions was varied at constant segment–segment interactions and chain molecular weight. We have used surface-energy measurements and X-ray photoelectron spectroscopy (X.p.s.) to study the surface composition and obtain information on the concentration–depth profile. The compatibility of the blend constituents was studied by monitoring the melting-point depression[18] of the PEO phases and by constructing the phase diagrams of ternary systems PEO/MMAS/$CHCl_3$. Finally, the results are discussed in the context of Binder's mean-field treatment[1].

EXPERIMENTAL

Materials

Random poly(methyl methacrylate-*co*-styrene) copolymers (MMAS) were prepared by free-radical polymerization in toluene with 2,2'-azobis(2-methylbutyronitrile) as initiator (0.4% w/w) at 120°C. The molecular weight and polydispersity index of the copolymers (*Table 1*) were determined by gel permeation chromatography (g.p.c.) with tetrahydrofuran (THF) as the carrier and with polystyrene standards calibration. Copolymer composition was confirmed by ^{13}C n.m.r. The copolymers were carefully precipitated from toluene into petroleum spirits and dried under vacuum at 60°C overnight. PS, PMMA and PEO homopolymers were supplied by Aldrich and used as received (*Table 1*).

Phase diagrams

Phase diagrams of PEO/MMAS/chloroform ternary systems were constructed by titrating heterogeneous mixtures across the blend composition range with chloroform until they became clear at room temperature.

Surface energy

The surface energy was determined from the advancing contact angles (θ) of two probe liquids, distilled water and methylene iodide, on 100 μm thick films of the blends, by means of the harmonic mean approximation:

$$(1+\cos\theta)_i\gamma_i = 4\left(\frac{\gamma_i^d\gamma_s^d}{\gamma_i^d+\gamma_s^d}+\frac{\gamma_i^p\gamma_s^p}{\gamma_i^p+\gamma_s^p}\right) \quad (1)$$

Superscripts d and p correspond to the dispersive and polar components of the surface energy, respectively; subscripts i and s denote the probe liquid and solid, respectively. The surface energy of water and methylene iodide was measured as 72.6 and 50.8 dyn cm^{-1}, respectively. The dispersive and polar components were 50.5 and 22.1 dyn cm^{-1} for water and 44.1 and 6.7 dyn cm^{-1} for methylene iodide. By rewriting equation (1) for the two probe liquids, we obtain a system of two equations with two unknowns, γ_s^d and γ_s^p. Contact angles (θ) were determined by the Wilhelmy plate technique at 20°C by means of the Cahn dynamic contact-angle analyser (DCA, model 312) at a speed of 94 $\mu m\ s^{-1}$. The procedure involved measurement of the advancing contact angles of water and methylene iodide on films of the blends coated on rectangular microscope glass coverslips that were dried at 60°C under vacuum overnight. The technique consists of monitoring the force exerted on the sample during immersion and emersion in a probe liquid at a constant speed by means of an electronic balance. The contact angle is determined from the force (F) corrected for the buoyancy force (force at zero depth of immersion), the perimeter of the sample and the surface energy of the probe liquid. Data were collected over at least 15 mm depth of sample immersion in the probe liquid, hence providing contact angles averaged over a large sample surface area. This alleviates problems associated with surface heterogeneity on macroscopic scale (millimetres) encountered with the traditional method of contact-angle determination. The contact-angle data together with the relevant information for the two probes were used to calculate the surface energy of the films at room temperature using equation (1).

Table 1 Molecular weights and polydispersity indices of homopolymers and copolymers

Polymer	Styrene (%)	$\bar{M}_n$ ($\times 10^3$)	$\bar{M}_w/\bar{M}_n$
PS	100	119.6	3.6
MMAS95	95	21.5	2.8
MMAS90	90	24.0	2.4
MMAS80	80	15.3	3.1
MMAS60	60	22.4	2.8
MMAS40	40	18.6	2.5
MMAS20	20	17.0	2.8
MMAS0	0	100.0	2.5
PEO	–	46.4	2.0

X-ray photoelectron spectroscopy

X.p.s. spectra were recorded with a Kratos XSAM800 photoelectron spectrometer fitted with a Mg/Al dual X-ray gun and a DS800 data system. Typical operating conditions were as follows: X-ray source, 12 kV, 25 mA; pressure in the source chamber, 4×10^{-9} Torr. Angular-dependent X.p.s. measurements were carried out by rotating the samples relative to the analyser by an angle θ of 0°, 45° and 80°.

Differential scanning calorimetry

About 5 mg of sample were accurately weighed in pierced, crimped aluminium pans and tested by means of a Du Pont 912 dual cell calorimeter at 10°C min^{-1} under nitrogen atmosphere. Thermograms were recorded with the samples as cast from room temperature to 150°C.

Sample preparation

Films were prepared by solution casting from dilute (5% w/v) solutions in chloroform at room temperature. Residual solvent was removed under vacuum at 60°C over 15 h.

RESULTS AND DISCUSSION

Surface composition by surface-energy measurements

We have used the surface energies calculated from equation (1) to determine the surface composition in terms of the fractional coverage of the top 10 Å by each blend constituent. *Figure 1a* shows a typical surface energy *versus* composition graph. The total surface energy of a

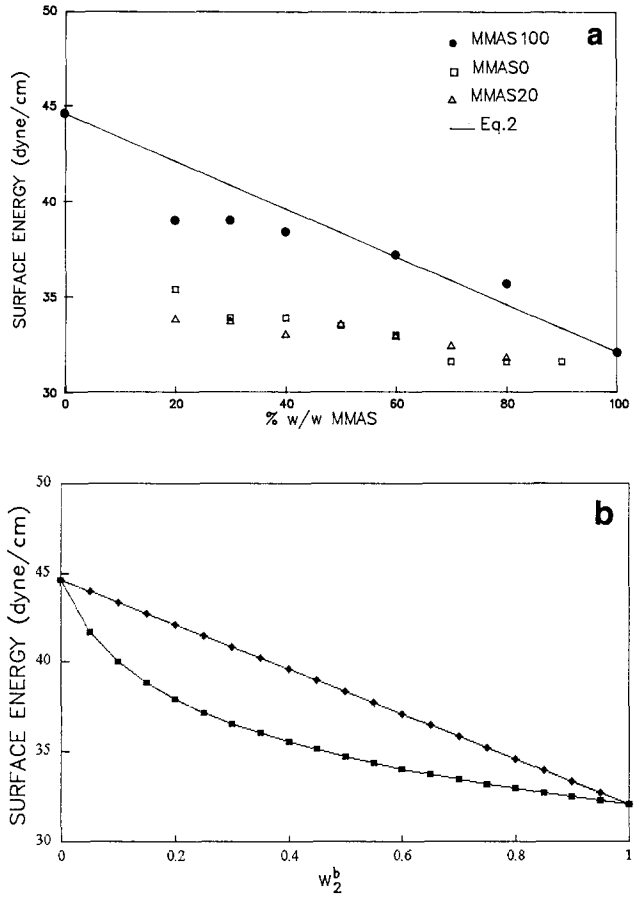

Figure 1 (a) Surface energy (γ) *versus* blend composition. (b) Comparison of the surface-energy variation with blend composition for a homogeneous and a heterogeneous blend using equations (6) (the Belton–Evans equation, ■) and (2) (weight average, ◆), respectively ($M_1 = M_2$, $\alpha_s = 100$ Å^2)

heterogeneous multicomponent system, γ, can be related to its surface composition through the surface fraction, f_i^s, of each component:

$$\gamma = f_1^s \gamma_1 + f_2^s \gamma_2 \quad (2)$$

Equation (2) neglects any free-volume effects and specific interactions assuming a heterogeneous surface. Rearrangement of equation (2) yields the surface fraction, f_1^s, surface weight fraction, w_1^s, and distribution coefficient, k_1:

$$f_1^s = (\gamma - \gamma_2^\circ)/(\gamma_1 - \gamma_2) \quad (3)$$

$$w_1^s = f_1^s \rho_1 / [f_1^s \rho_1 + (1 - f_1^s)\rho_2] \quad (4)$$

$$k_1 = w_1^s / w_1^b \quad (5)$$

where ρ is the density; superscripts s and b denote surface and bulk properties, respectively.

In the case of a homogeneous system, the surface composition can be related to the total surface energy by the Belton–Evans equation[19], developed for binary liquid systems that form perfect solutions:

$$\gamma = \gamma_1^\circ + (kT/\alpha_s) \ln\{d/[1 + (d-1)x_1]\} \quad (6)$$

where $d = \exp[\alpha_s(\gamma_2^\circ - \gamma_1^\circ)/kT]$, γ_1° is the surface energy of pure component 1 and α_s is the area occupied by a single chain at the interface. *Figure 1b* compares equations (2) and (6) for a blend of two polymers with equal molecular weights and α_s of 100 Å^2. The differences between the two curves arise from the compatibility between the two polymers, and must be taken into account to avoid misinterpretation of surface-energy data in homogeneous systems.

We have used equation (3) to determine the surface composition of our blends, hence implicitly assuming a heterogeneous surface. This is justified for our systems. Use of equation (3) in the case of the one bulk homogeneous system (PEO/PMMA) would perhaps provide an overestimate for the concentration of the lower-surface-energy component at the surface. It is, however, justified from the semicrystalline nature of our blends, which, even in the case of the homogeneous systems, would present a surface consisting of amorphous and crystalline regions.

Homopolymer blends, PEO/PS and PEO/PMMA

The surface energy of PEO, PMMA and PS homopolymers was 44.6, 32.1 and 35.2 dyn cm^{-1}, respectively. The surface energy of MMAS copolymers varied between 32 and 35 dyn cm^{-1}. The surface-energy differential between the components of the PEO/PS and PEO/PMMA blends was 13 and 9.4 dyn cm^{-1}, respectively. The surface composition of the PEO/PMMA blends was slightly enriched in PMMA when prepared by the standard casting procedure (*Figure 2*). The PEO/PS blend presented an air interface depleted in PS (*Figure 2*). When the films were annealed at temperatures above the glass transition temperature of the two homopolymers and the melting point of PEO, 170°C for 3 h, the PEO/PS blend surface was significantly enriched in PS whereas that of the PEO/PMMA blends showed more subtle changes (*Figure 2*). Blends with PMMA as the minor component showed a slight enrichment in the PMMA, which disappeared on phase inversion. Changes in the PEO/PMMA blends were close to the experimental error of the technique. It is worth pointing out that the surface composition for the PEO/PMMA blend was calculated with equation (2), that is, assuming some form of heterogeneity at the air interface. In the case of a completely homogeneous surface, the data would, in view of equation (6), tend to indicate no enrichment or depletion of the PMMA from the air interface. At any rate, however, the surface would not be enriched in PMMA to any significant extent as in the case of PEO/PS.

Blends of PEO with MMAS copolymers

The surface composition of blends of PEO with MMAS copolymers varied with copolymer composition (*Figure 3*). Incorporation of styrene in the copolymer, in amounts as low as 2% w/w, resulted in surface enrichment of the blend surface in the copolymer. The extent of surface coverage seemed to increase with styrene content in the copolymer. Bearing in mind that the surface-energy differential for all systems remained almost constant, the cause of this behaviour must be related to the extent of compatibility between the two blend components.

Compatibility of PEO with MMAS copolymers

It is well established in the literature that PEO is compatible with PMMA[13–16] and incompatible with PS[17]. We have studied the compatibility of MMAS copolymers with PEO in terms of the ternary phase diagrams and the PEO melting-point depression.

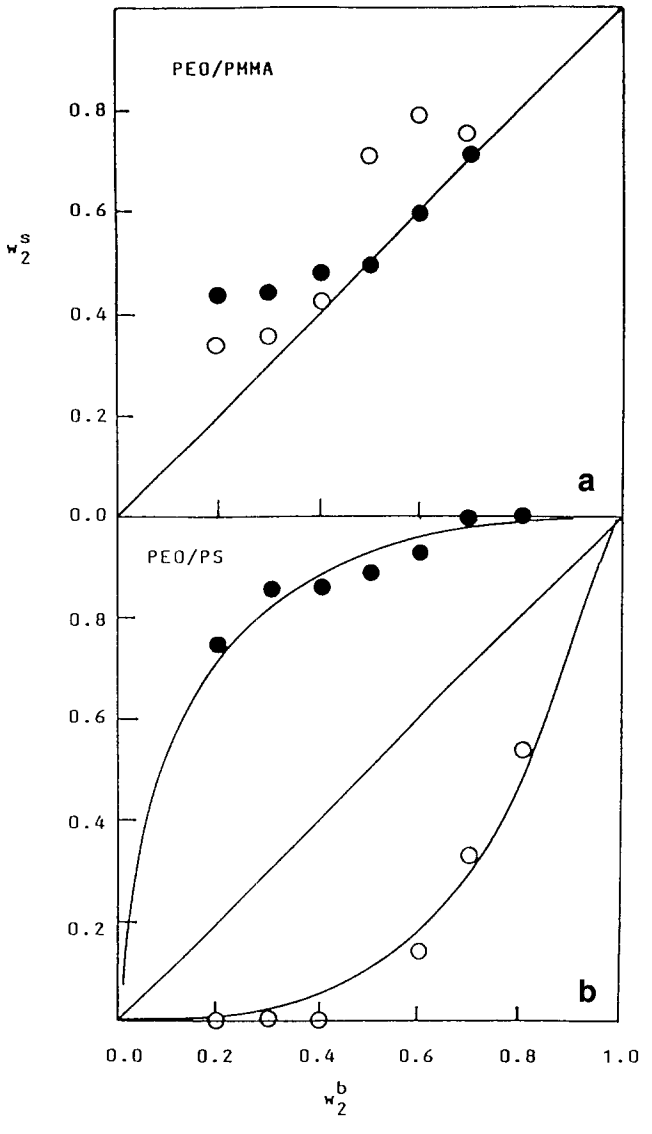

Figure 2 Effect of blend composition and annealing on surface enrichment in (a) PEO/PMMA and (b) PEO/PS blends before (○) and after (●) annealing at 170°C. w_2^s = weight fraction of PMMA or PS at the air interrface; w_2^b = weight fraction of the same polymers in the bulk

Styrene had a significant effect on the binodal of the ternary system PEO/MMAS/$CHCl_3$, as shown in *Figure 4*. The binodal shifted to lower polymer concentrations with increasing styrene content in the copolymer, indicating increasing incompatibility. The binodals were not symmetrical, suggesting preferential solubility of the copolymer in $CHCl_3$, compared to PEO. The variation of the extent of the incompatibility with copolymer composition has been conveniently expressed in terms of the plait polymer–polymer interaction parameter (equation (7));

$$\chi_{23}^{pl} = 0.5(x_2^{-0.5} + x_3^{-0.5})\,(1-\phi_1^{pl})^{-1} \qquad (7)$$

where x is the number of polymer segments and ϕ_1^{pl} is the solvent volume fraction at the plait point; subscripts 2 and 3 correspond to PEO and MMAS copolymers, respectively. χ_{23}^{pl} increased three-fold as the styrene content increased from 5 to 95% w/w (*Figure 5*).

Melting-point depression

The extent of incompatibility in semicrystalline polymer blends is related to the melting-point depression[18,20] of the crystalline component:

$$T_m^{-1} - (T_m^\circ)^{-1} = -\frac{RV_2}{\Delta H_2 V_1}\chi_{12}(1-\phi_2)^2 \qquad (4)$$

where ΔH_2 is the heat of fusion per mole segment, V is the molar volume and T_m° the equilibrium melting point; subscripts 1 and 2 denote the amorphous and crystalline polymer, respectively. *Figure 6* shows the variation of the melting point of the PEO-rich phases with increasing copolymer and styrene contents. The behaviour of the PEO/copolymer blends was contained between two extremes defined by the PEO/PMMA and PEO/PS systems. In the case of PEO/PMMA compatible system, the melting point decreased monotonically with increasing PMMA content. Incorporation of MMA monomer units

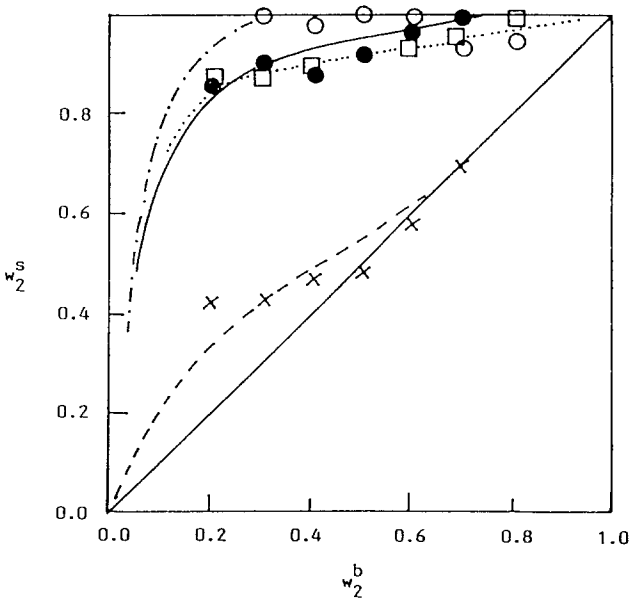

Figure 3 Effect of blend composition and MMAS copolymer composition on surface enrichment in PEO/MMAS blends: (○) MMAS80; (□) MMAS20; (×) PMMA; (●) MMAS2. Copolymer compositions are listed in *Table 1*

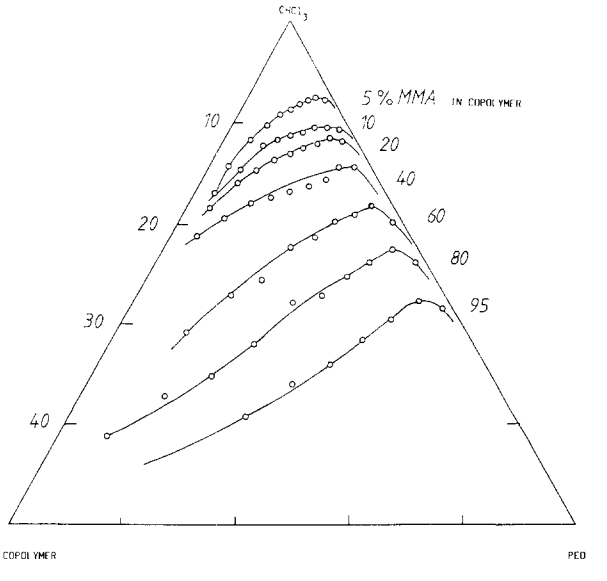

Figure 4 Phase diagram of PEO/MMAS/$CHCl_3$ blends with varying MMAS copolymer composition

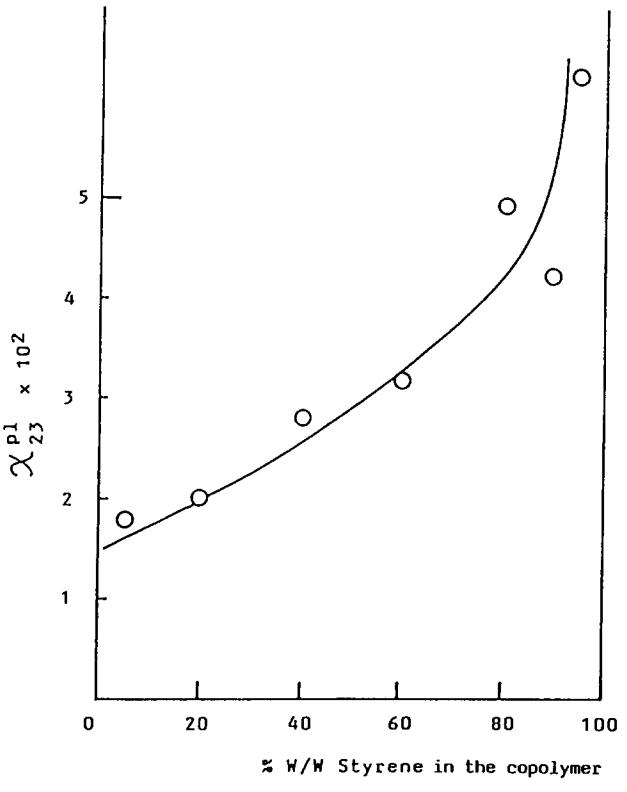

Figure 5 Effect of copolymer composition on blend χ_{23}^{pl}

in the PS chain produced an inflection in the $T_m(\phi)$ curve, which shifted to lower copolymer concentrations with increasing MMA content in the copolymer. The level of the plateau-like region, at low copolymer content, shifted to lower temperatures for the intermediate copolymer compositions (10–95% styrene). A value of -0.13 was calculated for the PEO–PMMA interaction parameter at 60°C, in agreement with literature data[14,15].

X.p.s. analysis

X-ray photoelectron spectroscopy (X.p.s.) has been used extensively in the study of surfaces of polymer blends[21]. Quantitative analysis of the X.p.s. data takes advantage of the linear relationship between the integrated intensity (I_i) of a core-electron photoemission spectrum and the average number of atoms per unit volume, N_i:

$$I_i \simeq S_i N_i \tag{9}$$

The sensitivity of atoms in distinct chemical environments is assumed constant, allowing calculation of the atomic ratio from the intensity ratio. Our analysis concentrated on the C(1s) and O(1s) spectra. A straight line was fitted as the baseline using Wagner sensitivity factors. The atomic ratios obtained from equation (9) were converted to weight fractions. As a result of the chamber pressure, 10^{-8} Torr, a finite layer of hydrocarbon was deposited on the specimen surface during measurements. This was accounted for in our calculations by incorporating an appropriate correction. By changing the photoelectron take-off angle to the analyser, a concentration–depth profile can be obtained. The sampling depth is given by:

$$z \simeq 3\lambda \cos\theta \tag{10}$$

where θ is the take-off angle and λ is the mean free path for electrons escaping from the surface. The sampling depth assumes its maximum value, $z \simeq 3\lambda$, at take-off normal to the surface. A value of 23 ± 3 Å was assigned to λ, based on the work by Clark and coworkers[22].

Figure 7 compares the behaviour of two MMAS copolymers, 80/20 and 20/80 w/w MMA/S, before and after annealing, at $\theta = 0°$, corresponding to a depth of 69 ± 9 Å. Both systems showed depletion in MMAS prior to annealing. Annealing increased the amount of copolymer on the top 69 Å for both systems. The

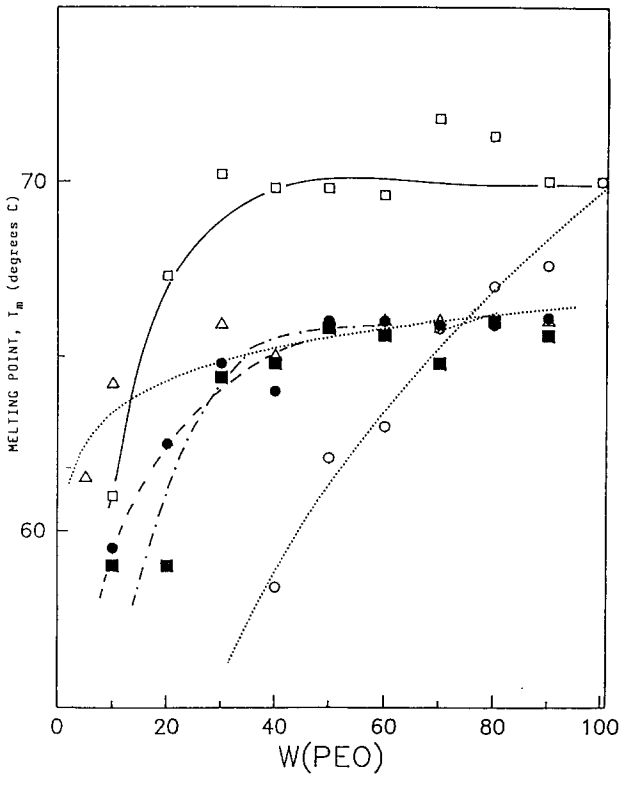

Figure 6 Variation of T_m with copolymer composition, W(PEO) = PEO weight fraction: (○) 100% MMA; (□) 5% MMA; (△) 10% MMA; (●) 20% MMA; (■) 30% MMA

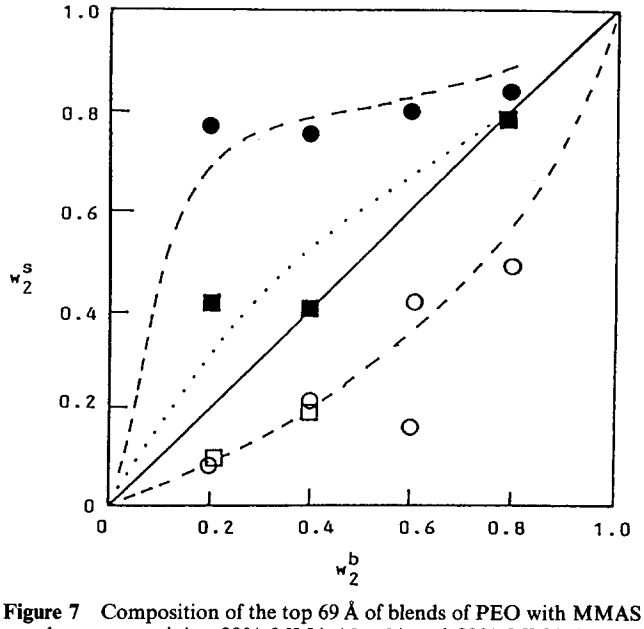

Figure 7 Composition of the top 69 Å of blends of PEO with MMAS copolymers containing 20% MMA (○, ●) and 80% MMA (□, ■) before (○, □) and after (●, ■) annealing at 170°C

Table 2 X.p.s. data for 60/40 w/w PEO/MMAS80

θ (deg)	z (Å)	w_2^a	conditions
0	69	0.43	As cast
45	49	0.48	As cast
80	12	0.55	As cast
0	69	0.76	Annealed
80	12	0.90	Annealed

[a] Data corrected for hydrocarbon contamination; $w_2^b = 0.40$

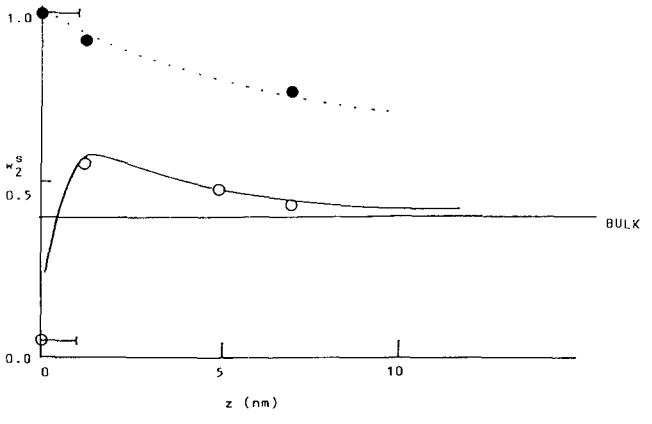

Figure 8 Integral composition profile of a 60:40 w/w PEO/MMAS blend before (○) and after (●) annealing at 170°C. The dotted curve represents the mean-field prediction (equation (13)). z = distance from the air interface

surface composition of the system with 80/20 MMA/S approached the bulk composition, but that with 20/80 MMA/S showed a significant surface enrichment of MMAS.

The sample 60/40 w/w PEO/MMAS80 was selected for depth profiling before and after annealing. Significant surface enrichment required annealing (*Table 2*), in agreement with the surface-energy measurements. The surface-energy and X.p.s. data are shown in a single graph (*Figure 8*), illustrating the integral surface composition profile. The data point at $z=0$ was obtained from the surface-energy measurements. The error bar corresponds to the root-mean-square radius of gyration for the average MMAS copolymer chain calculated from Flory's equation[20]. The annealed specimen showed the typical hyperbolic decay of the MMAS concentration approaching its bulk value. Significant enrichment persisted at 69 Å from the surface. The untreated sample showed depletion of the very top layer of the air interface in MMAS, quickly assuming its bulk concentration.

Mean-field modelling of depth profile

For a blend of a homopolymer (component 3) and a random copolymer (components 1 and 2), the interaction parameter is given[23] by:

$$\chi_{blend} = \chi_{13}\phi_1 + \chi_{23}\phi_2 - \phi_1\phi_2\chi_{12} \qquad (11)$$

where ϕ_1 and ϕ_2 denote the volume fraction of component 1 and 2 in the copolymer, respectively. The polymer–polymer interaction parameters are available in the literature:

$$\chi_{13} = +0.221$$
$$\chi_{12} = -0.127\ (60°C)$$
$$\chi_{23} = +0.040\ (60°C)$$

Subscripts 1, 2 and 3 correspond to PEO, PMMA and PS, respectively. According to *Figure 9*, incorporation of MMA in the copolymer chain does not lead to compatible systems until MMA contents in excess of 60% w/w in amorphous systems (60°C). Although this is an overestimate in view of the d.s.c. data, it indicates a monotonic decrease of χ with MMA content in the copolymer.

We have used polymer–polymer interaction parameters quoted in the literature to predict the surface enrichment depth profile in our systems. The model used was based on the mean-field treatment proposed by Schmidt and Binder[1] for partially compatible linear flexible polymers in the presence of a selective wall. In agreement with Cahn's[24] original observations, they showed that at the two-phase coexistence curve the wall is always 'wet' by a macroscopically thick layer of the preferred phase. As the system moves along the coexistence curve towards the two-phase region, it undergoes a 'wetting transition' from the wet state, characterized by a macroscopic surface layer, to a non-wet state, where the thickness of the surface layer is small. The concentration profile, given by:

$$z = (\alpha/6)\, d\phi / \{\phi(1-\phi)[G(\phi,\chi) - G(\phi_\infty,\chi) - \Delta\mu(\phi-\phi_\infty)]\}^{0.5} \qquad (12)$$

is exclusively determined by the bulk properties of the blend, blend composition (ϕ_∞), free energy per site G and the chemical potential difference $\Delta\mu$. In the case of a partially wet surface, the concentration profile can be approximated by an exponential decay[1,25] with the bulk correlation length, ζ_b, as the decay length:

$$\phi(z) = \phi_1^b + (\phi_1^s - \phi_1^b)\exp(-z/\zeta_b) \qquad (13)$$

where postscripts b and s denote the bulk and surface, respectively. It has been successfully used in the case of blends of polystyrene/deuterated polystyrene by Jones and coworkers[12,13].

The bulk correlation length, ζ_b, of a Flory–Huggins blend is given by:

$$\zeta_b = (\alpha/6)\phi_1^b(1-\phi_1^b)(\chi-\chi_s)^{-0.5} \qquad (14)$$

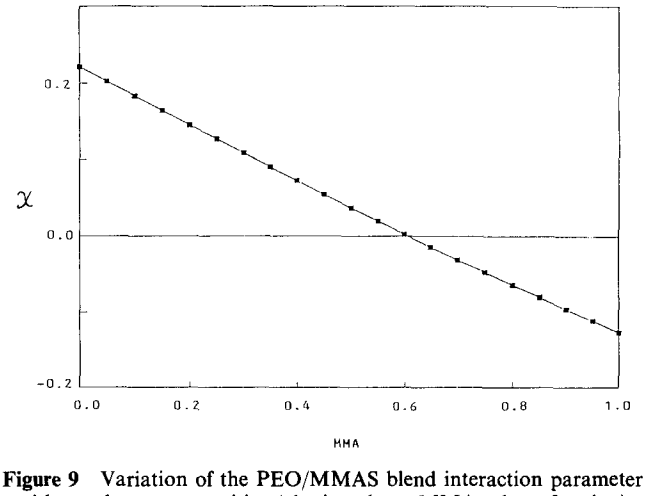

Figure 9 Variation of the PEO/MMAS blend interaction parameter χ with copolymer composition (abscissa shows MMA volume fraction)

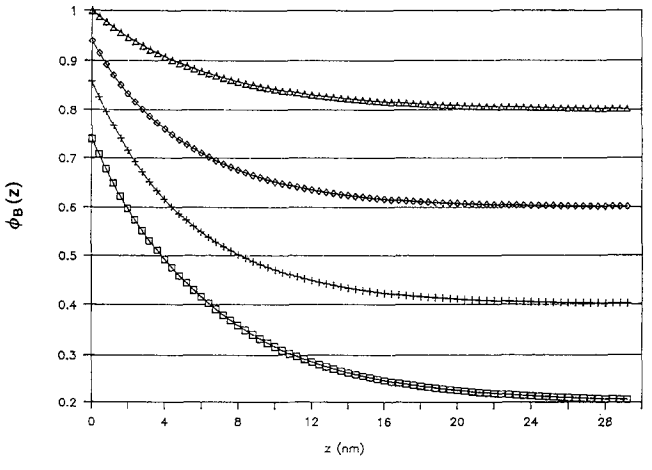

Figure 10 Depth profile for PEO/PS (A/B) blend calculated from the mean-field treatment (equation (13)), with $\chi_{AB}=0.221$: (□) $\phi_B^b=0.2$; (+) $\phi_B^b=0.4$; (◇) $\phi_B^b=0.6$; (△) $\phi_B^b=0.8$. ϕ_B^b is the bulk volume fraction of lower-surface-energy polymer

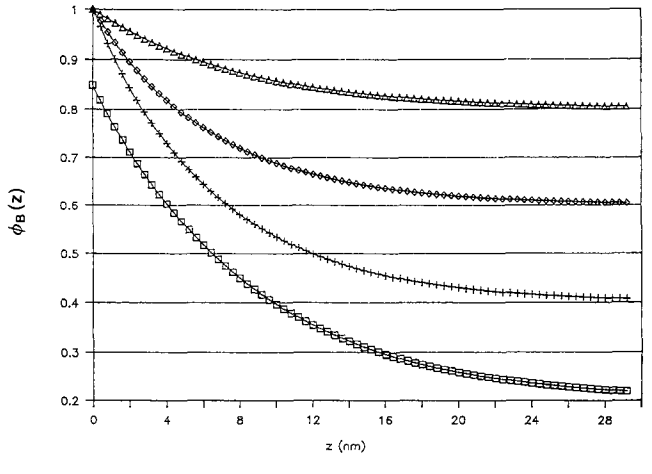

Figure 11 Depth profile for PEO/MMAS40 (A/B) blend calculated from the mean-field treatment (equation (13)), with $\chi_{AB}=0.146$: (□) $\phi_B^b=0.2$; (+) $\phi_B^b=0.4$; (◇) $\phi_B^b=0.6$; (△) $\phi_B^b=0.8$. ϕ_B^b is the bulk volume fraction of lower-surface-energy polymer

The lattice spacing, α, was calculated from Kuhn step length (σ) and the root-mean-square radius of gyration of the two chains:

$$\sigma_1=\sigma_2=\sigma=\langle R_{gyr}^2\rangle^{1/2}(6/N)^{1/2} \quad (15)$$

$$a=(\sigma_1^2\phi_1+\sigma_2^2\phi_2)^{1/2} \quad (16)$$

The polymer–polymer interaction parameter at the spinodal was calculated from[26]:

$$\chi_s=0.5\{(N_1\phi_1)^{-1}+[N_2(1-\phi_1)]^{-1}\} \quad (17)$$

The composition profiles are generated from equation (12) using the surface composition determined from the surface-energy measurements.

Figures 10 and *11* demonstrate calculations for two blends with varying blend composition. Blends of PEO with PS produced exponential depth profiles extending down to 25 nm. Incorporation of 20% by weight MMA in the copolymer did not alter the basic shape and characteristics of the profile, but this time the profile reached down to 28–30 nm. It is interesting to note that the available experimental points of the concentration profile are in excellent agreement with the mean-field prediction (*Figure 8*). The simulation confirms that careful control of the extent of incompatibility between blend constituents is required for maximum concentration profile depth. The beneficial contribution from increased incompatibility in terms of surface coverage can have a detrimental effect on the depth of the concentration profile. This is in agreement with the expected growth of the enriched layer thickness as we approach the coexistence curve, $\Delta\mu\rightarrow 0$. It must be emphasized that this analysis does not take into account the semicrystalline nature of our systems and it is, therefore, indicative of the basic trends in the corresponding amorphous system.

DISCUSSION

The results reported in this paper suggest that the incompatibility between blend constituents has a strong influence on the extent of surface coverage and the depth of concentration profile. Although this is in agreement with earlier observations made with PCL/PVC blends[7], it is *apparently* inconsistent with data reported by Koberstein and coworkers on PS/PVME in the homogeneous region of the phase diagram[11]. Before we attempt to rationalize the experimental data, we discuss the general molecular mechanism for surface enrichment in polymer blends.

A pure liquid containing a single species will minimize its total surface free energy by keeping its total surface area to a minimum. This is implemented by an inward attractive force exerted on the surface molecules. The surface free energy can be altered only through reorientation of the molecules at the surface, so that the ends of the largest force field point inwards. This is not the case for mixtures of two species with different strength of attractive force fields per unit area. The molecules with the strongest attractive force fields will tend to diffuse into the bulk, leading to a depleted surface profile. Let us now consider a fluid mixture of two species with low (**1**) and high (**2**) surface energy. According to the previous argument, the lower-surface-energy species, **1**, will enrich the surface, forming, say, a monomolecular layer. The propensity of the bulk molecules **1** to locate near this surface monomolecular layer will be both enthalpy- and entropy-controlled in the case of small species. In the case of high-molecular-weight polymers, entropy will be negligible, hence this process will be controlled to a significant extent by the enthalpic interactions, **1–2**, **2–2** and **1–1**.

Our data suggest that, despite the significant surface-energy differential, the homogeneous blend, PEO/PMMA, did not produce any surface enrichment in the lower-surface-energy component, in contrast to the heterogeneous blend, PEO/PS. This is a result of the compatibility between the blend constituents and the crystallization of the PEO-rich phases. In the case of the compatible blend, PEO/PMMA, the PEO crystallized during film casting and the lower-surface-energy component, PMMA, remained trapped in the bulk through favourable enthalpic interactions with PEO. In the opposite case, the lower-surface-energy component, PS, phase-separated out of the blend during solvent evaporation, migrating to the air interface at equilibrium conditions following annealing at 170°C. The question is: Why doesn't PMMA also diffuse to the air interface to any significant extent during annealing? This, at present,

is not fully understood. It is perhaps a result of the magnitude of the χ parameter of that system compared to systems like PS/PVME and the presence of crystallization. The χ parameter of the former system is -0.127 compared to -1×10^{-4} for PS/PVME[11]. This would render the favourable enthalpic interactions between the blend constituents considerably weaker in PS/PVME compared to PEO/PMMA, accounting for the lack of surface enrichment in the latter blend. The available data do not afford a comprehensive explanation of the contribution of PEO crystallization to the surface enrichment. It would be reasonable to postulate that crystallization is a more powerful process compared to phase separation. The implication would be that, in the case of a compatible system, the lower-surface-energy component will be subjected to a significant drive to remain within the crystallizable PEO-rich phases. In the opposite case, the lower-surface-energy polymer will be rejected strongly from the forming PEO spherulites.

ACKNOWLEDGEMENTS

The author is grateful to Miss A. Lane for experimental assistance and Mr Neil Malone for the very skilful X.p.s. analysis.

REFERENCES

1 Schmidt, I. and Binder, K. *J. Physique* 1985, **46**, 1631
2 Nakanishi, H. and Pincus, P. *J. Chem. Phys.* 1983, **79** (2), 997
3 Thomas, H. R. and O'Malley, J. J. *Macromolecules* 1979, **12**, 323
4 O'Malley, J. J., Thomas, H. R. and Lee, G. M. *Macromolecules* 1979, **12**, 996
5 Thomas, H. R. and O'Malley, J. J. *Macromolecules* 1981, **14**, 1316
6 Schmitt, R. L. and Gardella, J. A., Jr *Macromolecules* 1986, **19**, 648
7 Clark, M. B., Jr, Burkhardt, C. A. and Gardella, J. A., Jr *Macromolecules* 1991, **24**, 799
8 Schmidt, J. J., Gardella, J. A., Jr and Salvati, L., Jr *Macromolecules* 1989, **22**, 4489
9 Kang, S. K. and John, M. S. *J. Colloid Interface Sci.* 1991, **144**, 390
10 Maejima, M., Takeda, Y., Inoue, T. and Sakai, T. *Sen-I Gakkaishi* 1988, **44**, 60
11 Bhatia, Q. S., Pan, D. H. and Koberstein, J. T. *Macromolecules* 1988, **21**, 2166
12 Jones, R. A. L., Kramer, E. J., Rafailovich, M. H., Sokolov, J. and Schwarz, S. A. *Phys. Rev. Lett.* 1989, **62**, 280
13 Jones, R. A. L. and Kramer, E. J. *Phil. Mag. (B)* 1990, **62**, 129
14 Liberman, S. A., Gomes, A. De S. and Macchi, E. M. *J. Polym. Sci., Polym. Chem. Edn.* 1984, **22**, 2809
15 Cortazar, M. M., Calahorra, M. E. and Guzman, G. M. *Eur. Polym. J.* 1982, **18**, 165
16 Ito, H., Russell, T. P. and Wignall, G. D. *Macromolecules* 1987, **20**, 2213
17 Olabisi, O., Robeson, L. M. and Shaw, M. T. 'Polymer–Polymer Miscibility', Academic Press, New York, 1979
18 Nishi, T. and Wang, T. T. *Macromolecules* 1975, **8**, 909; Kwei, T. K., Nishi, T. and Roberts, R. F. *Macromolecules* 1974, **16**, 391
19 Belton, J. W. and Evans, M. G. *Trans. Faraday Soc.* 1946, **41**, 1
20 Flory, P. J. 'Polymer Chemistry', Cornell University Press, Ithaca, NY, 1956
21 Briggs, D. and Seah, M. P. 'Practical Surface Analysis by Auger and X-Ray Photoelectron Spectroscopy', Wiley, New York, 1983
22 Clark, D. T. and Thomas, H. R. *J. Polym. Sci., Polym. Chem. Edn.* 1977, **15**, 2843
23 ten Brinke, G., Karasz, F. E. and MacKnight, W. J. *Macromolecules* 1983, **16**, 1827
24 Cahn, J. W. *J. Chem. Phys.* 1977, **66**, 3667
25 Binder, K. and Frisch, H. L. *Macromolecules* 1984, **17**, 2928
26 de Gennes, P. G. 'Scaling Concepts in Polymer Physics', Cornell University Press, Ithaca, NY, 1979